Density functional theory of structural transformations of oxygen-deficient centers in amorphous silica during hole trapping: Structure and formation mechanism of the E′ _γ·

Uchino, Takashi

Yoko, T.

(Citation)
Physical Review B,74(12):125203-125203

(Issue Date)
2006-09

(Resource Type)
journal article

(Version)
Version of Record

(URL)
https://hdl.handle.net/20.500.14094/90000238

Density functional theory of structural transformations of oxygen-deficient centers in amorphous silica during hole trapping: Structure and formation mechanism of the E'_γ center

T. Uchino
Department of Chemistry, Faculty of Science, Kobe University, Nada, Kobe 657-8501, Japan

T. Yoko
Institute for Chemical Research, Kyoto University, Uji, Kyoto 611-0011, Japan

(Received 17 March 2006; revised manuscript received 3 August 2006; published 18 September 2006)

We investigate the hole trapping process of a neutral oxygen vacancy in amorphous silicon dioxide (a-SiO_2) using cluster calculations based on the density functional theory (DFT) method. We show that trapping a hole at a neutral oxygen vacancy leads to the formation of several types of positively charged defects. One immediate consequence of the hole trapping process at the oxygen vacancy site is the creation of the positively charged dimer, in which a unpaired electron is almost equally distributed over the two Si aoms in the defect. Our calculations further demonstrate that the dimer configuration can be transformed into other minimum energy structures. Three possible relaxation channels are likely to exist, leading to the three distinctive defect configurations called the puckered, forward-oriented, and bridged hole-trapping oxygen-deficiency center (BHODC) configurations. To evaluate the stability of these positively charged defects against discharging, we then calculate the electrical levels for all the positively charged clusters investigated here. It is shown that the BHODC configuration has the highest electrical level, implying that this type of positively charged defect is the most stable configuration against electron trapping. We also calculate the hyperfine parameters and g values of the BHODC using the DFT method. The calculated hyperfine parameters and g values are in good agreement with those observed for the E'_γ center. These results corroborate our previous attribution of the E'_γ center [Uchino and Yoko, Phys. Rev. Lett. **86**, 5522 (2001)].

DOI: 10.1103/PhysRevB.74.125203 PACS number(s): 61.72.Ji, 61.43.Fs, 68.35.Dv

I. INTRODUCTION

Photoinduced electronic excitation of amorphous solids is primarily followed by the formation of electrons, holes, and excitons near the band edge states. Among other electronic excitation processes in amorphous materials, charge carrier trapping in amorphous silicon dioxide (a-SiO_2) induced by ionizing radiation has attracted considerable interest because the trapping properties of a-SiO_2 strongly affect the performance and reliability of insulating oxide layers used in metal oxide semiconductor (MOS) devices.[1] In addition, recent advances in fiber Bragg grating devices used in silica-based optical waveguides are indebted to the photoinduced change in refractive index called the photorefractive effect.[2] Thus, the trapping of photoinduced carriers and the consecutive structural modifications in a-SiO_2 have attracted much attention during the past decades.

By electrical measurements, it is possible to obtain information about the charge state of a radiation-induced defect. The charge state of a defect in thin oxide layers is evidenced by a shift in characteristic voltages of MOS devices. The measured voltage shift demonstrated that thin-film a-SiO_2 tends to become positively charged during ionizing radiation or hole injection, indicating that a certain defect in the oxide layer actually behaves as a hole trap.[3] It has been well recognized from the combination of electron paramagnetic resonance (EPR) and electrical measurements[4] that the principal positively charged defect center in a-SiO_2 is the E'_γ center,[5,6] which is ascribed to an unpaired electron in a dangling tetrahedral orbital of a three-coordinated silicon atom with near axial symmetry. Thus, any good model of hole trapping in a-SiO_2 must successfully explain the structure and formation mechanism of the E'_γ center as well. However, the question concerning the mechanism of hole trapping process in a-SiO_2 along with the formation and structure of the E'_γ center still remains to be solved.

It was once generally assumed that the microscopic structure of the E'_γ center in a-SiO_2 is basically identical to that of the E'_1 center in α quartz because the EPR characteristics of these two types of E' centers are very similar.[7] The accepted model of the E'_1 center in α quartz, which was originally given by Feigl, Fowler, and Yip (FFY),[8] can be viewed as a positively charged and asymmetrically relaxed oxygen monovacancy. According to the FFY model, an unpaired electron is localized in the sp^3 orbital of one of the silicon atoms in the oxygen monovacancy, whereas a hole is trapped at the silicon atom on the other side of the vacancy. This hole trapping reaction can be written by $\equiv Si—Si\equiv + h^+ \rightarrow \equiv Si\cdot + {}^+Si\equiv$. This structure can further relax through the plane of the three neighboring oxygens and then forms a puckered configuration with a nearby back oxygen atom [see Fig. 1(a)].[9]

In view of the EPR characteristics, it is indeed true that "there seems to be no reason not to assume that E'_γ in glass is essentially identical with the E'_1 center in α quartz," as was pointed out by Griscom.[10] However, this is not necessarily true for the electrical properties. As mentioned earlier, the charge state of the E'_γ center was shown to be positive from the electrical measurements. It is also interesting to note that the charge state of the E'_γ is rechargeable.[11,12] That is, the positive charge of the E'_γ center can be discharged to the neutral and EPR invisible state by electron injection under

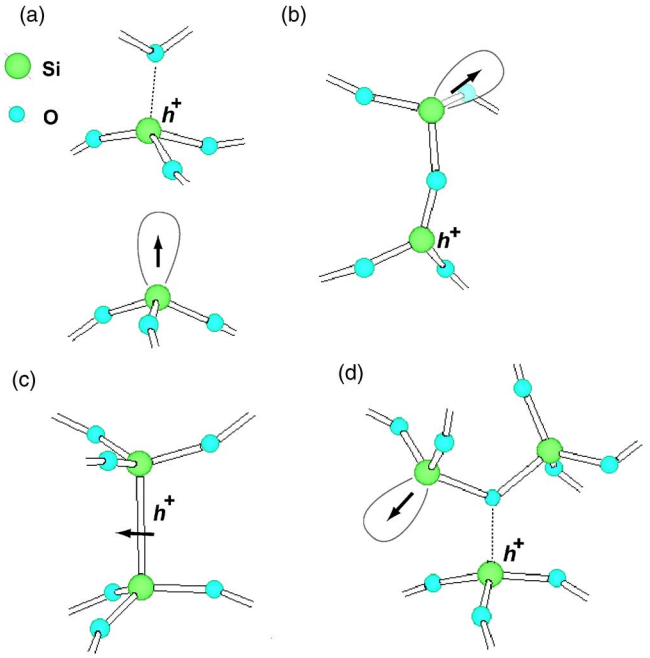

FIG. 1. (Color online) Schematic illustration of the positively charged defect centers investigated in this work: (a) Conventional puckered configuration; (b) bridged hole-trapping oxygen-deficiency center (BHODC); (c) dimer configuration; (d) forward-oriented configuration.

positive bias, and essentially equal number of E'_γ centers and positive charges are generated again by the subsequent hole injection process under negative bias,[12] showing a switching behavior. These results appear to indicate that there is little permanent structural change at the hole trapping site after subsequent electron capture.[13] In other words, the resulting neutral site is able to recharge in response to changes in the voltage applied to the system. However, such rechargeablility against applied electric fields is not expected to occur in the FFY model of the E'_γ center because the electron capture at the $\equiv Si\cdot + {}^{+}Si\equiv$ site will lead to the original oxygen monovacancy site, $\equiv Si—Si\equiv$, which will be inert against applied voltages unless accompanied by ionizing radiations.[11] Thus, as far as the E'_γ-center model in silica glass is concerned, the FFY model that will involve any permanent change after an electron capturing event may need to be reevaluated, as has been previously implied by Warren *et al.*[13]

Furthermore, it has recently been recognized that the FFY model or a relevant puckered configuration is not the only configuration that can account for the basic experimental feature of the E'_γ center in a-SiO_2.[14–17] Thus far, there have been several attempts to predict microscopic structures of the E'_γ center using different theoretical approaches,[18–20] and a couple of new structural models have been proposed.[14,15] It should be noted, however, that the models proposed in Refs. 14 and 15 are more or less based on the FFY model and give no explanation for the switching behavior of the E'_γ center.

In our recent papers,[16] we have also put forward an alternative model of the E'_γ center using *ab initio* quantum-chemical cluster calculations. Our model consists of a threefold coordinated silicon with an unpaired electron ($\equiv Si\cdot$) and a threefold coordinated silicon with a hole ($\equiv Si^{+}$) similar to the case of the FFY model, but these two types of Si centers share a common oxygen atom to form an oxygen-bridged structure $=(Si\cdot)—O—(Si^{+})=$. We called this defect structure as a bridged hole-trapping oxygen-deficiency center [BHODC, see Fig. 1(b)]. One of the possible precursors of this charged defect is a neutral epoxidelike structure, $=Si\overset{\cdots}{\underset{O}{\_\_}}Si=$, which we called a triangular oxygen deficiency center (TODC).[16] We have further shown that our newly proposed model can account for several previously unexplained characteristics of the E'_γ center, including a switching phenomenon,[21] the capture of diffusing O_2 and H,[16] and the related luminescence behaviors.[22] Recently, independent support for our model was given by Alemany and Chelikowsky[23] by using different *ab initio* techniques.

Although our newly proposed model may capture some basic experimental characteristics of the E'_γ center, it appears that this model gives any insight into the hole trapping process at a neutral oxygen vacancy, $\equiv Si—Si\equiv$, which will certainly be a major vacancy site in a-SiO_2. In this paper, we hence perform a series of *ab initio* cluster calculations to investigate the fate of the hole trapped at the $\equiv Si—Si\equiv$ defect and show that this vacancy site can also become a precursor of the BHODC structure. More interestingly, we will show that the electrical level of this bridged configuration is substantially higher than that of the conventional positively charged puckered configuration, illustrating the more stability of BHODC against discharging. We further calculate the hyperfine parameters and g values of BHODC and demonstrate that the calculated values are in good agreement with those observed for the E'_γ center, further corroborating our structural attribution of this paramagnetic center.

This paper is organized as follows. Models and methods of calculations are given in Sec. II. Section III describes the structure and energies of various neutral and positively charged oxygen vacancies. In Sec. IV, the structure and stability of the positively charged defects pertaining especially to the E'_γ center are discussed in terms of the electrical levels, hyperfine parameters, and g values. The conclusions are given in Sec. V.

II. MODELS AND CALCULATIONAL PROCEDURES

In this work, a cluster approach based on the *ab initio* molecular orbital method is used to model the local structure of various oxygen vacancy defects in a-SiO_2 and the relevant hole-trapping processes. It has been well recognized that *ab initio* quantum-chemical calculations give highly accurate results concerning the structure, energies, and electronic properties of isolated molecules.[24] This method has been further applied to solids to calculate their electronic and vibrational properties using a cluster approach. It should be noted, however, that the cluster method should only be used to calculate the localized electronic states since this approach cannot fully take into account the actual effect of condensed environments. Thus, cluster approaches have been mainly devoted to the characterization of the electronic structure of point defects in crystalline and amorphous materials.[19,25,26]

This is based on the assumption that the electronic states associated with point defects are rather localized and do not extend through the corresponding solid.

Even in the case of the calculations of point defects in solids, however, it would be preferable to employ larger clusters. In particular, larger models will be necessary in investigating the structural transformation of a defect, which will accompany the atomic rearrangements not only of a defect itself but also of its surrounding atoms in the medium-range length scale. To overcome the problem of a conventional cluster approach, Shluger *et al.*[27,28] have recently proposed a atomistic embedding technique which combines a quantum-chemical treatment of a defect and its surrounding with the classical shell-model treatment. This embedding technique is intriguing in that it can take account of a full dielectric and mechanical representation of the infinite solids.

Although the effect of the electrostatic potential of the solid cannot be fully taken into account, we here use a conventional cluster approach based on the state-of-the-art density functional theory (DFT) calculations, which allow one to obtain several important electron paramagnetic resonance (EPR) properties, e.g., hyperfine parameters and g values, in good accuracy. To include the effect of the surrounding dielectric medium as possible as we can and we employ model clusters as large as possible within the limitation of our computer time.

In this work, we constructed the model clusters having an oxygen vacancy according to the following procedures. First, we obtained a stoichiometric or a nondefective cluster consisting of 31 Si and 46 O atoms; the cluster is so constructed as to consist of five- and six-membered rings, which are major ring components in a-SiO_2.[29] The surface Si atoms in the cluster are terminated by H atoms to tie up the surface related dangling bonds. Thus, the stoichiometry of the cluster can be described as $Si_{31}O_{46}H_{32}$. The geometry of the stoichiometric cluster was fully optimized at the DFT level. To create a neutral-oxygen-vacancy site, we intentionally removed one oxygen atom that is located almost in the center of the cluster and reoptimized the structure without imposing any structural constraints.

On the basis of the above procedures, we constructed two isomers of $Si_{31}O_{45}H_{32}$ both having a neutral oxygen vacancy (see Fig. 2). As shown in Fig. 2, two isomers have different connectivity of the constituent SiO_4 tetrahedra; one of the isomers, termed model I, has two back oxygen atoms behind the oxygen vacancy site, whereas the other, termed model II, does not. We employed these two types of clusters as a model of the neutral oxygen vacancy in a-SiO_2 because, unlike the case of α quartz, the vacancy site in the amorphous silica network will not necessarily have back-oxygen atoms.

To mimic an ionization process related to the oxygen vacancy defect, we reoptimized the structure of models I and II by simply assuming a total charge of +1, resulting in the positively charged "dimer" configuration (see Fig. 3). To search other local minimum structures of the positively charged defect, we then intentionally changed the coordinates of several atoms around the defect and performed geometry optimization starting from such a modified configuration. As a result, several defect structures that are substantially different from the dimer configuration were obtained. It should also be noted that some configurations have been shown to have lower total energies than the dimer configuration. The details of the calculated results will be given in the next section.

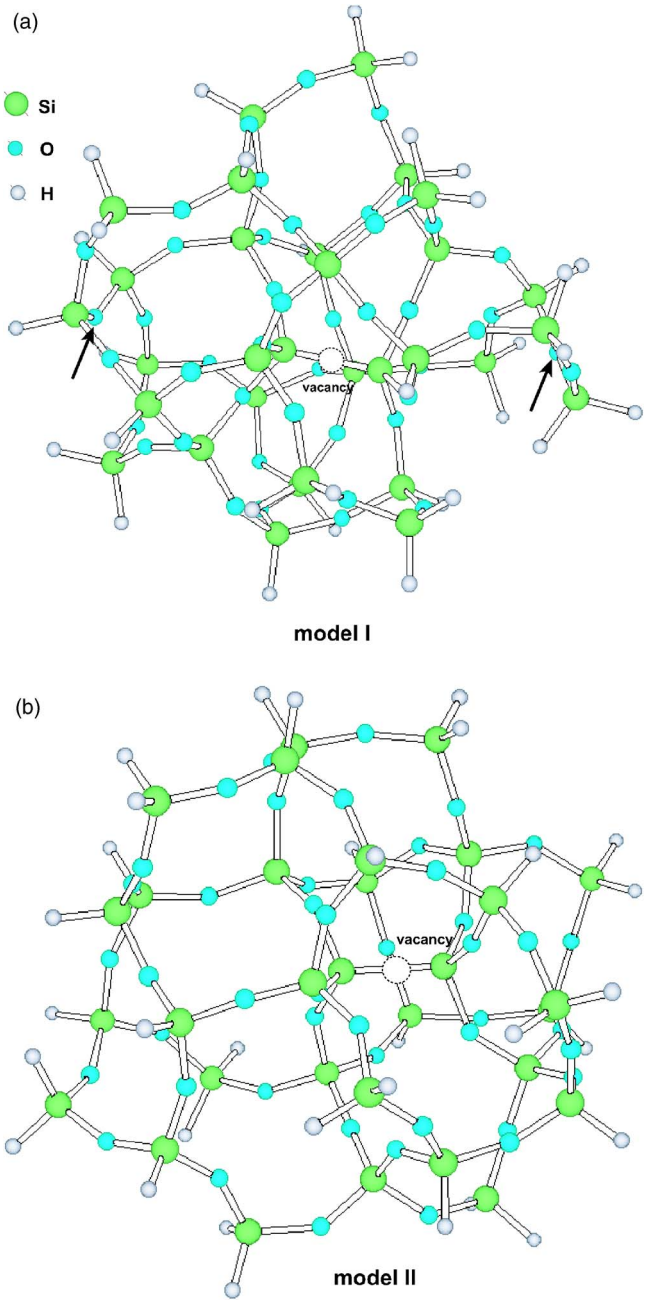

FIG. 2. (Color online) Two different model clusters of atoms ($Si_{31}O_{45}H_{32}$) with a neutral-oxygen-monovacancy employed in this work: (a) model I, two back oxygen atoms are indicated by arrows; (b) model II.

In this work, all *ab initio* quantum-chemical calculations have been done at the DFT levels with the 6-31G(d) basis set[30] using the GAUSSIAN 03 computer program.[31] For the DFT calculations, we employed the B3LYP exchange-correlation functional consisting of the Lee-Yang-Parr correlation functional[32] in conjunction with a hybrid exchange functional proposed by Becke.[33]

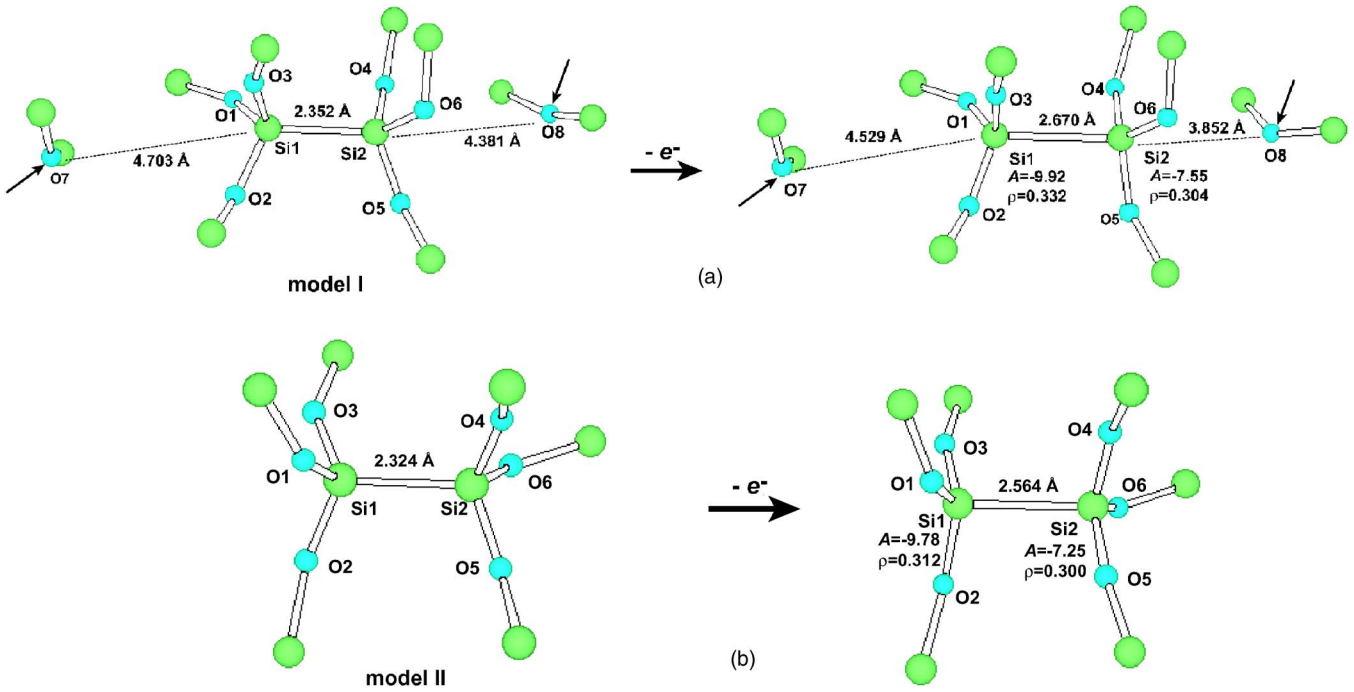

FIG. 3. (Color online) Moiety of the clusters modeling a neutral oxygen vacancy shown in Fig. 2 and its corresponding positively charged dimer configuration: (a) model I, two back oxygen atoms are indicated by arrows; (b) model II. Geometry optimizations were performed at the B3LYP/6-31G(d) level. Principal bond distances (in Å), spin densities, and hyperfine coupling constants (in mT) are also shown.

III. RESULTS

A. Structure of a neutral oxygen vacancy and a positively charged dimer configuration

The whole optimized structure of two neutral off-stoichiometric clusters, namely model I and model II, is shown in Fig. 2. Figure 3 highlights the defect part of the clusters and shows some optimized bond distances related to the defect. The positively charged dimer configurations derived from models I and II are also shown in Fig. 3. As has been reported previously,[18,19] the Si-Si bond in the oxygen vacancy site is weakened after trapping a hole and a remaining unpaired electron is delocalized between the two Si atoms in the defect, forming a dimer configuration. The calculated isotropic hyperfine coupling constants of the two paramagnetic silicons in models I and II are $\sim 8 - \sim 10$ mT (see Fig. 3), which are in reasonable agreement with those obtained from previous cluster calculations.[19,16]

B. Formation of the back-puckered configuration

It has been recognized that the positively charged dimer structure is metastable and can be relaxed to some lower energy forms of the defect.[15,18,19] It is hence interesting to investigate possible lower or minimum energy configurations using the present cluster approaches.

One of the previously recognized lower energy structures is the puckered FFY configuration[9] mentioned in the Introduction. The asymmetric relaxation of the dimer accompanied by puckering most likely result from the strong interaction between the positively charged puckering silicon atom (Si_P^+) and the back oxygen atom (O_B). When the stabilization energy due to this interaction exceeds the delocalization energy of an unpaired electron in the dimer configuration, the defect will be transformed into the puckered configuration. It should be noted, however, that the severe puckering of Si_P^+ will induce unfavorable strain on the network around the defect. This implies that not all of the dimer configuration will relax into a puckered configuration, but a part of the defect sites having O_B in their neighborhood will accept the Si_P^+-O_B interaction. Mukhopadhyay *et al.*[15] estimated from their recent embedded cluster method that the number of sites capable of accommodating puckered configurations does not exceed 10% and the resultant asymmetric structure is governed by the initial atomic configurations around the dimer. The results reported by Mukhopadhyay *et al.*[15] demonstrates that the stabilization energy due to puckering depends strongly on the surrounding atomic environment around the dimer.

In our previous calculations using small cluseters,[16] we tried to obtain the puckered configuration starting from a dimer configuration. However, we did not obtain any puckering of the positively charged Si atom; the symmetric dimer configuration was always produced even when we started from a highly asymmetric positively charged configuration.[16] From these calculated results, we suggested that at the charged oxygen vacancy site there exists only a single potential well that leads to the symmetric dimer configuration. We should note, however, that, as also pointed out in Ref. 34, this result may be applied only to the case in which a back oxygen was missing and/or not properly located.

In the present larger model, the dimer in model I has two O_B atoms behind the respective Si atoms [see Fig. 3(a)]. It is, hence, expected that the puckered configurations are ob-

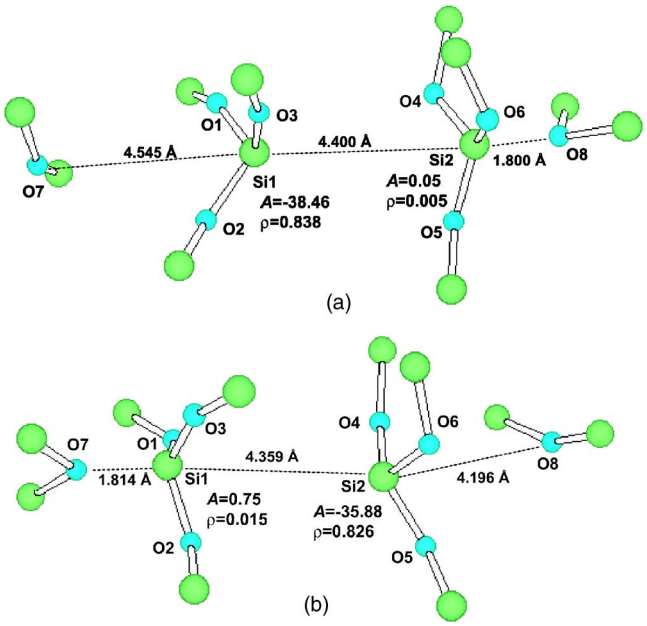

FIG. 4. (Color online) Two configurations of the positively-charged puckered defect derived from model I. Geometry optimizations were performed at the B3LYP/6-31G(d) level. Principal bond distances (in Å), spin densities, and hyperfine coupling constants (in mT) are also shown.

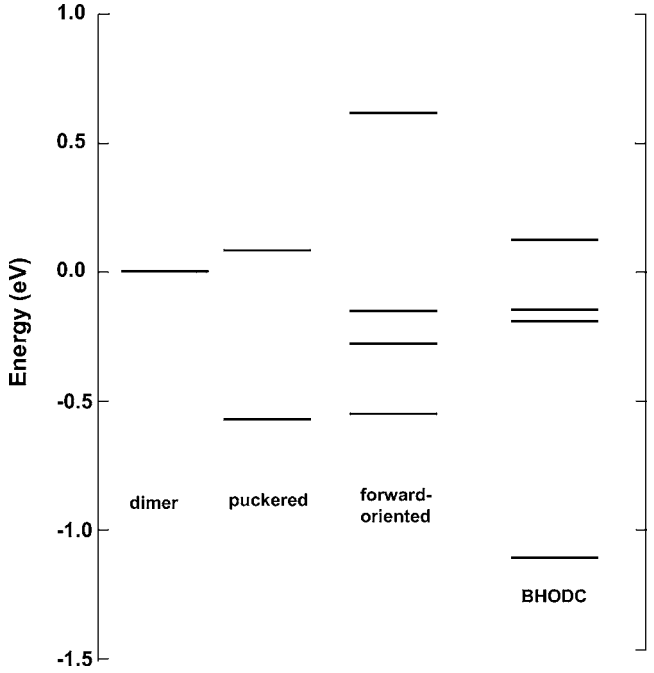

FIG. 5. Total energies of all the positively charged clusters employed in this work. The calculations were performed at the B3LYP/6-31G(d) level. As for the energies of the puckered, forward-oriented, and TODC clusters, the energy of the corresponding dimer cluster is referenced to 0 eV.

tained even in our cluster models. To induce such a possible asymmetric relaxation, we shifted the position of each Si atom in the dimer to the nearest O_B atom by 0.3–0.5 Å and then performed geometry optimization by using the intentionally deformed configurations. As a result, we found that such deformed configurations lead to an asymmetric relaxation, resulting in the puckered configurations. When the initial position of the Si2 (or Si1) atom in model I was so shifted as to interact with the back O8 (or O7) atom, the resultant positively charged cluster lead to the configurations shown in Fig. 4(a) [or Fig. 4(b)]. The total energy of cluster shown in Fig. 4(a) is lower than that of that shown in Fig. 4(b) by 0.66 eV. (See also Fig. 5.) This energy difference between the two puckering configurations probably results from the difference in the atomic environments behind the Si_P^+ atoms in the respective clusters. It should also be noted that the higher energy form of the cluster shown in Fig. 4(b) is even higher in total energy than the positively charged dimer by 0.085 eV, demonstrating that the puckered configurations are not necessarily energetically favored as compared with the original dimer configuration. As for the lower energy form of the cluster shown in Fig. 4(a), however, its total energy is lower than that of the dimer configuration by 0.57 eV, which is in reasonable agreement with the values estimated previously for the puckered configuration in α quarts estimated by cluster 0.64 eV (Ref. 19), embedded cluster 0.4 eV (Ref. 35), and supercell calculations [0.4 eV[18] 0.6 eV (Ref. 14)] The present calculations hence show that the energy stabilization obtained by puckering depends strongly on the surrounding environments of the defect center. This is basically in harmony with the results obtained by Mukhopadhyay *et al.*[15]

As for model II, the puckered and related dangling-bond configurations were not obtained even if we start from a highly asymmetric defect configuration during the optimization process, in agreement with our previous calculations using small clusters.[16]

C. Formation of the forward-oriented configuration

As mentioned in the previous section, the driving force to induce the asymmetric relaxation of the dimer will be a strong electrostatic force between the Si_P^+ and O_B atoms. We would like to mention, however, that the back oxygen atom may not be the only oxygen atom that can interact with the positively charged Si atom in the dimer; rather, a "forward" oxygen (O_F) is also expected to interact with the charged Si atom, resulting in an asymmetric relaxation similar to the case of the conventional puckered configuration. The possibility of such a "forward-oriented" configuration was previously pointed out in our previous paper[34] to account for the interconversion between the $\equiv$Si—Si$\equiv$ bond and the two-fold coordinated divalent Si atom ($=$Si:) upon ionizing radiation. In Ref. 34, we have shown from cluster calculations that one of the Si atoms in the dimer can interact with one of the three oxygen atoms that are bonded to the rest of the Si atom in the dimer, forming the lower-energy forward-oriented configuration shown in Fig. 1(d). When the positive charge of the forward-oriented configuration is neutralized by capturing an electron, the defect configuration does not go back to the original neutral oxygen vacancy but to the divalent Si atom, giving a theoretical account for the $\equiv$Si—Si$\equiv \rightleftarrows =$Si: interconversion during ionizing radia-

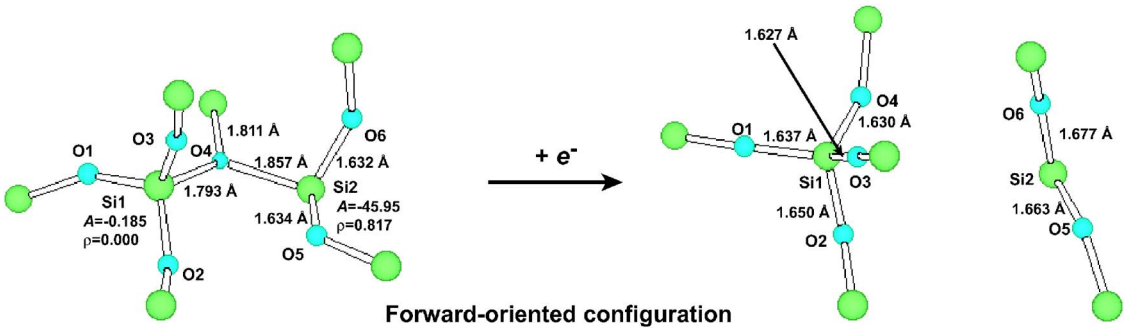

FIG. 6. (Color online) An example of the forward-oriented configurations (left) and the corresponding neutral species (right) obtained in this series of cluster calculations. Geometry optimizations were performed at the B3LYP/6-31G(d) level. Principal bond distances (in Å), spin densities, and hyperfine coupling constants (in mT) are shown.

tion exposure.[34] This interconversion process was also confirmed by Donadio, Bernasconi, and Boero[36] using *ab inito* molecular dynamics simulations.

In this work, we will also explore the above relaxation process that leads to the forward-oriented configuration using the present cluster models. To search the equilibrium configuration associated with the positively charged forward-oriented Si (Si_{FO}^{+}) atom, we intentionally induced the interaction between one of the Si atom in the dimer and its nearby O_F. That is, the position of one Si atom in the neutral $\equiv$Si—Si$\equiv$ defect in model I or model II is shifted to the direction of a nearby O_F atom by ~0.4 Å, and the geometry of this cluster is fully optimized by assuming the total charge of +1. In this work, we selected several different sets of Si_{FP}^{+} and O_F atoms in model I or model II to induce such a forward-oriented interaction.

As a result of the geometry optimization, we actually found that the forward-oriented relaxations are possible to occur for different sets of Si_{FP}^{+} and O_F atoms. Figure 6 shows an example of the optimized configurations. We have found that the unpaired electron is almost localized at a single Si atom in the forward-oriented defect configurations (see, for example, Fig. 6). Figure 5 shows the relative total energies of four isomers having different forward-oriented configurations derived from model I or model II. We see from Fig. 5 that the calculated total energy of the optimized clusters depends on the set of Si_{FP}^{+} and O_F atoms employed to induce the forward-oriented relaxation. This indicates that the total energy of these clusters is affected by the surrounding environment around the defect, similar to the case of the puckered configurations mentioned in Sec. III B.

It is interesting to note that in inducing forward-oriented relaxation there is no need to assume the presence of any particular atoms around the defect since forward oxygens are always located in front of each Si atom in the dimer. On the other hand, the conventional puckering is allowed to occur only at a restricted dimer site where a back oxygen is properly located behind the dimer to accommodate puckering. Unfortunately, we did not evaluate the energy barrier for the transitions from the dimer to puckered and forward-oriented configurations in the present cluster approach because the reaction coordinates involved in these transitions are rather complex. However, the present cluster calculations will give theoretical evidence that the forward-oriented configurations are not far from realistic in considering the transformations of the positively charged dimer structure.

D. Formation of the bridged hole-trapping oxygen-deficiency center

In the preceding sections, we have shown that the dimer configuration can relax into the puckered and/or forward-oriented configurations. In this section, we will demonstrate that the forward-oriented configuration can further be transformed into the structure called the bridged hole-trapping oxygen-deficiency center, BHODC, shown in Fig. 1(b).

In the forward-oriented configuration, the forward oxygen O_F is coordinated by three Si atoms. We have found that all the three O_F—Si bonds have rather long bond distances (~1.8 Å) as compared with the normal Si—O bond (~1.62 Å) in the silica network. This implies that the bonding character of the O_F—Si bonds is substantially weakened as a result of the interaction between Si_{FP}^{+} and O_F. It is hence expected that these weakened Si—O_F bonds tend to be ruptured, which may allow further atomic rearrangements. One possible atomic rearrangement is the bond switching shown in Fig. 7, leading to the transformation from the forward-oriented configuration to the BHODC configuration. On the basis of the concept, the atomic positions related to the forward-oriented configurations were so changed as to accomplish the bond switching depicted in Fig. 7. We then performed full geometry optimization using this modified configuration as an initial geometry by keeping the total charged of +1.

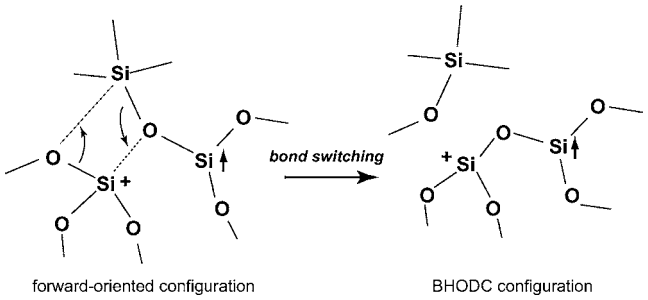

FIG. 7. Schematic illustration of the bond switching from the forward-oriented configuration to the bridged hole-trapping oxygen-deficiency center (BHODC).

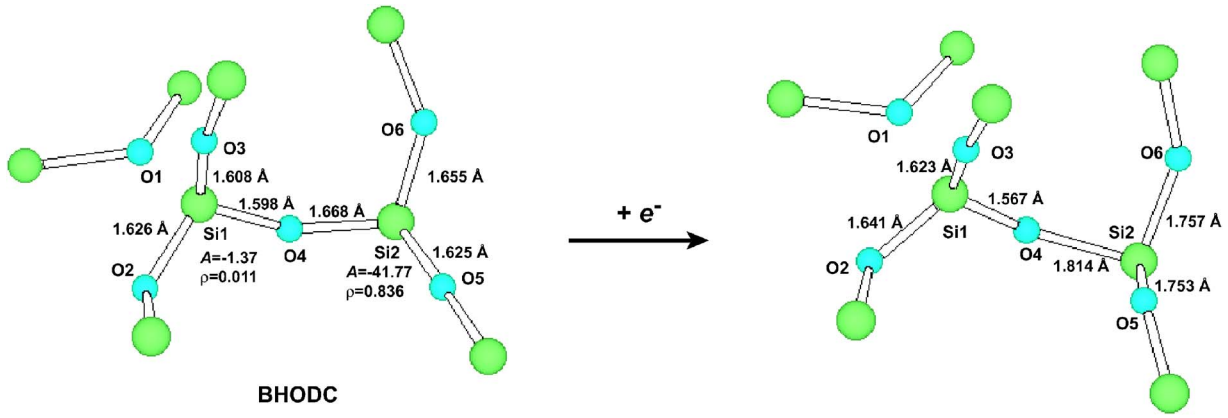

FIG. 8. (Color online) An example the BHODC configuration (left) and the corresponding neutral species (right) obtained in this series of cluster calculations. Geometry optimizations were performed at the B3LYP/6-31G(d) level. Principal bond distances (in Å), spin densities, and hyperfine coupling constants (in mT) are shown.

As a result, we have found that the BHODC structure shown in Fig. 1(b) is successfully reproduced. In this work, we obtained four different configurations of the BHODC structure derived from model I or model II. A typical example of the BHODC configuration is shown in Fig. 8. As in the case of the other positively charged clusters mentioned in the previous sections, one sees a distribution in total energy among the BHODC clusters (see also Fig. 5), also indicating that the total energy is affected by the surrounding environments of the defect center.

We also notice from Fig. 5 the total energies of the BHODC clusters are comparable to or even lower than those of the clusters modeling the dimer, puckered, and forward-oriented configurations, indicating that the BHODC configuration is not energetically unfavored.

The present cluster calculations hence demonstrate that as far as the total energy is concerned, none of the above defect configurations, i.e., dimer, puckered, forward-oriented, and BHODC configurations, are to be excluded as a model of the positively charged defect centers in a-SiO_2.

IV. DISCUSSION

A. Electrical levels

We have shown in Sec. III that trapping a hole at a neutral oxygen vacancy leads to the formation of various types of positively charged defects. We have also demonstrated that the total energy of the defect configurations depends strongly on the surrounding atomic arrangements. This is because the total energy includes not only the energy of the defect itself but also the strain energy around the defect, which may vary from site to site depending on the surrounding environments. Thus, judging from the total energy, we cannot tell which defect configuration is the most appropriate as a model of the thermally stable E'_γ center.

In actual a-SiO_2 the EPR signal related to the E'_γ center is completely bleached out as the temperature of the system is raised above ~800 K.[37] This indicates that the paramagnetic E'_γ center is eventually converted to a certain diamagnetic center by capturing an electron at such high temperatures. It is hence interesting to evaluate the stability of the respective defect centers against electron trapping. To evaluate the stability of the defect during charging and discharging events, we calculate the electrical level of the present defect centers. The electrical level is a measure of the energy involved in changing the charge state of a defect when both initial and final states of the system are in thermal equilibrium.[9,38,39] The lower the electric level is located, the more stable the corresponding neutral state becomes. In other words, the higher the electrical level, the more stable the positively charged state against electron capturing.

The electrical level is estimated from the total energy difference of two relaxed configurations of a cluster having different charges as follows:[9]

$$E(+/0) = E_{tot}(0) - E_{tot}(+) + \chi, \tag{1}$$

where $E_{tot}(n)$ is the total energy of the optimized configuration corresponding to the charge state n and χ is the electron affinity of SiO_2, which moves the reference energy from the vacuum level to the bottom of the conduction band. This definition hence gives the electrical level below the conduction band. We used the experimental value for χ (0.9 eV) according to previous studies.[9,38]

To calculate the electrical levels, we have to obtain the equilibrium configurations of the positively charged clusters after capturing an electron. For this purpose, we intentionally added one electron to the positively charged clusters, and then the structures were fully optimized starting from the configurations of the respective positively charged ones.

As for the dimer and puckered configurations, we found that these defects returned to the structures that are almost identical to the original neutral-oxygen-vacancy configuration upon capturing an electron. That is, the present calculations did not predict any puckered configurations in the neutrally charged state, in basically agreement with previous supercell calculations.[18,39] This indicates that the puckered configuration as well as the dimer configuration will spontaneously return to the original neutral-oxygen-vacancy form without any barrier or after overcoming a negligibly small barrier.

As for the forward-oriented and BHODC configurations, however, we obtained the structures that are different from the neutral-oxygen-vacancy configuration when the respective positively charged defects are given back an electron. We found that all the forward-oriented configurations are transformed into the divalent twofold coordinated Si structure upon capturing an electron (see Fig. 6), in agreement with our previous calculations using small clusters.[34,36] On the other hand, as shown in Fig. 8, the TODC has its own neutral form of the defect configuration, as has also been reported in our previous paper.[21] It appears that the neutral defect structure seen in Fig. 8 retains the basic defect configuration of BHODC, but one can find several crucial differences between the structure of the BHODC and its neutral form. For example, as shown in Fig. 8, all the three Si-O bonds associated with Si1 in the BHODC configuration have similar bond distances of ~1.6 Å, whereas, in its neutral form, the Si1-O4 bond is characterized by an exceptionally short bond distance (1.567 Å) as compared with the rest of the Si-O bonds related to Si1 (~1.62– ~1.64 Å), suggesting a higher bond order for the Si1-O4 bonding in the neutral configuration. Furthermore, the other side of the Si-O bond related to the O4 atom in the neutral defect, namely the Si2-O4 bond, has rather a long distance (1.814 Å) and hence may not be regarded as a normal siloxane bonding. From these calculated results, it is likely that the electron capturing process of the BHODC proceeds according to the following scheme:

$$=(\mathrm{Si}\bullet)\text{–}\mathrm{O}\text{–}(\mathrm{Si}^{+})= + e^{-} \rightarrow =(\mathrm{Si}\!:)^{-}\text{–}\mathrm{O}\text{–}(\mathrm{Si}^{+})= \rightarrow =\mathrm{Si}\!:\cdots{}^{-}\mathrm{O}\text{–}\mathrm{Si}^{+}=. \quad (2)$$

The $\mathrm{Si}:\cdots{}^{-}\mathrm{O}$ and $^{-}\mathrm{O}\text{-}\mathrm{Si}^{+}$ bonds on the far right side of Eq. (2) correspond respectively to the long and short Si-O distances seen in the neutral defect mentioned above.

Since we have obtained the optimized structures of the positively charged clusters and those of the corresponding neutral species, we can now estimate the electrical level $E(+/0)$. The calculated $E(+/0)$ values are shown in Fig. 9. As for the positively charged dimer and its neutral form, the electrical level was estimated previously by several researchers.[28,39] It is worth mentioning that the present calculated value (~−7.2 eV) is in reasonable agreement with those obtained previously from supercell calculations [−7.3 eV (Ref. 39)] and embedded-cluster calculations [−8.24 eV (Ref. 28)], showing that the present calculations yield a reasonable value for the electrical level although using an isolated cluster approach.

We notice from Fig. 9 that the electrical levels become higher in the order of dimer, puckered, forward-oriented, and BHODC configurations. This shows that the stability of the positively charged state against discharging increases in this order. We should note that the calculated values of the electrical levels are also affected by the surrounding environments around the defects. In the electrical-level calculations, however, the strain energies derived from the surrounding silica network are partially canceled out and that the calculations will yield the electrical levels due mainly to the defect of interest. We hence consider that the high-lying electrical level for the BHODC configuration results from rather a high total energy of the corresponding metastable neutral $=\mathrm{Si}:\cdots{}^{-}\mathrm{O}\text{-}\mathrm{Si}^{+}=$ configuration and that the high electrical level calculated for BHODC will rest inherently on this neutral species.

FIG. 9. Electrical levels calculated for the present model clusters related to the dimer, puckered, forward-oriented, and BHODC configurations. Levels are in eV referenced to the bottom of the conduction band of a-SiO_2.

From the foregoing calculations and discussion, we can conclude that the most stable form of the positively charged defects is the BHODC in terms of the electrical levels. The other forms of the positively charged defects such as the dimer, puckered, and forward-oriented configurations will be discharged earlier than the BHODC and will easily be transformed into the corresponding rather stable neutral configurations such as the neutral oxygen vacancy and the divalent Si (see Fig. 10). Once these stable neutral defects are formed, they will not be recharged just by injection of holes and electrons. As for the BHODC, however, the switching behavior is expected to occur between this positively charged state and the corresponding neutral $=\mathrm{Si}:\cdots{}^{-}\mathrm{O}\text{-}\mathrm{Si}^{+}=$ configurations in response to changes in the applied voltage because of the high electrical level (see also Fig. 10).

B. Model of the E'_γ center

Considering its high electrical level and the related switching behavior mentioned in the previous section, we suggest that the BHODC is the most probable candidate for the thermally stable form the E'-center variants, namely, the E'_γ center.

To give further theoretical support for the above model, we here calculate isotropic ^{29}Si hyperfine coupling constants and g values for the present positively charged clusters at the DFT-B3LYP/6-31G(d) level using the GAUSSIAN 03 code. It has previously been shown that the B3LYP hybrid functional can predict g values of small radicals with reasonable accuracy.[40]

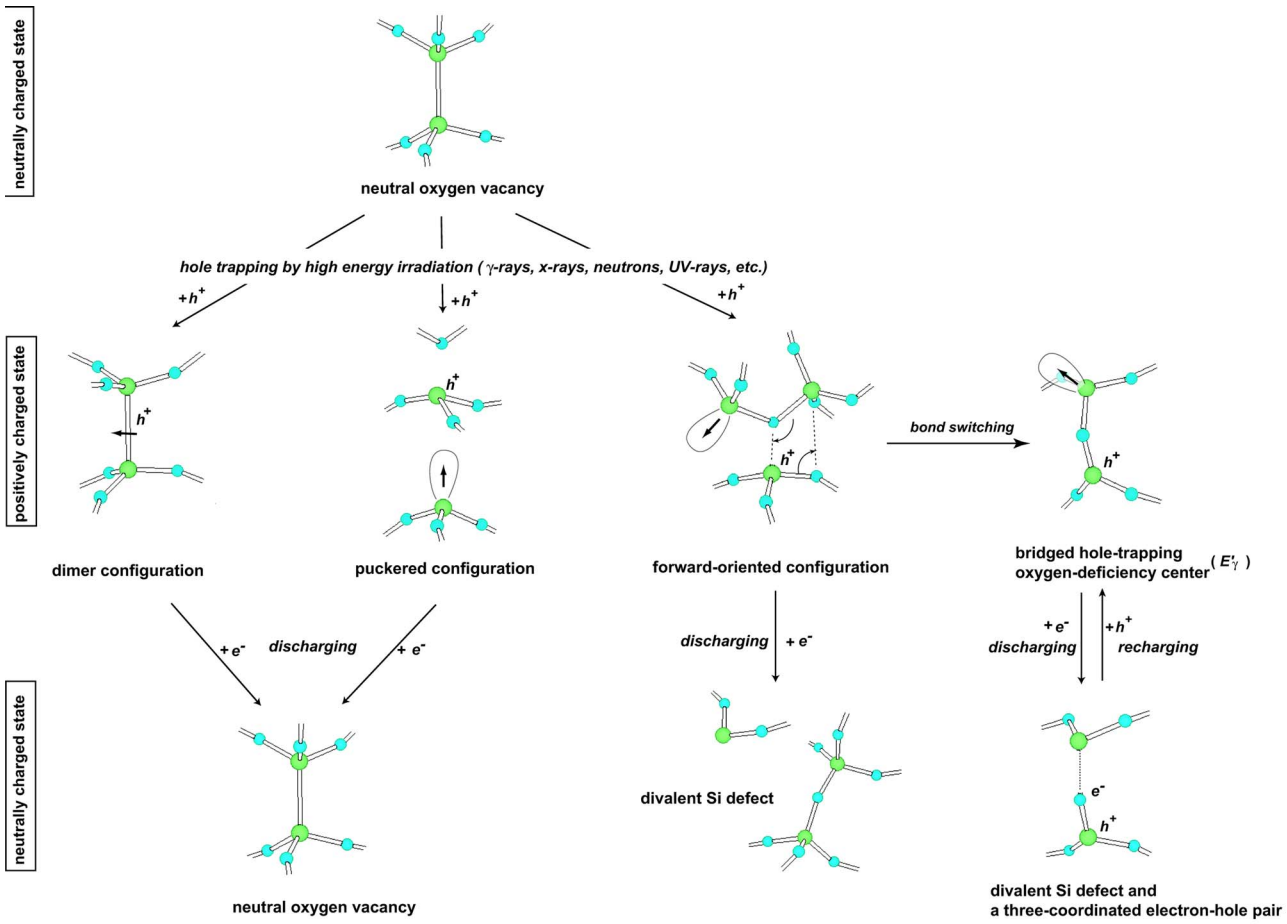

FIG. 10. (Color online) Possible relaxation channels of the neutral oxygen vacancy during the hole trapping and the subsequent discharging processes.

The results of hyperfine parameter and g value calculations for a series of clusters employed in this study are shown in Table I. Table I also shows the experimental spin Hamiltonian parameters observed for the E'_γ center. We see from Table I that the hyperfine parameters and g values calculated for the BHODC clusters are in good agreement with those observed for the E'_γ center. It should also be noted that the puckered configurations also yield the hyperfine constants and g values that are comparable to those of the E'_γ center. We, however, still propose that the BHODC structure is more pertinent to the microscopic origin of the E'_γ center than the back-puckered one because of the expected higher thermal stability of the former structure against discharging, as demonstrated in Sec. IV A. We admit that the formation of the BHODC structure requires rather complex structural rearrangements of the neutral oxygen vacancy during the hole trapping process as compared with the conventional puckering process. We should note, however, that the E'_γ center is induced by energetic radiations such as γ-rays,[6] x-rays,[6] and neutrons[41] or by the act of fiber drawing.[42] It is reasonable to expect that such energetic radiations and fiber drawing process will cause substantial atomic rearrangements around the oxygen vacancy defect. During ionizing radiation exposure, it is quite likely that a variety of hole-trapping centers, including dimer, puckered, forward-oriented, and BHODC configurations, are created. We should note, however, that

TABLE I. Results of g-value and hyperfine-parameter calculations for a series of positively charged clusters and comparison to the experimental results for the E'_γ center.

Type	g_1	g_2	g_3	$A_{iso}(^{29}Si)$
Expt.[a]				
E'_γ	2.0018	2.0006	2.0003	42
Calc.[b]				
dimer configuration	2.0023	2.0028	2.0028	−7.5, −9.8
	2.0023	2.0026	2.0031	−7.5, −9.9
puckered configuration	2.0020	2.0010	2.0004	−35.9
	2.0019	2.0006	2.0003	−38.5
forward-oriented	2.0019	2.0015	2.0000	−35.7
configuration	2.0022	2.0013	1.9996	−46.0
	2.0019	2.0011	1.9994	−42.1
	2.0019	2.0012	1.9994	−41.2
BHODC configuration	2.0019	2.0006	2.0000	−41.8
	2.0020	2.0006	2.0001	−43.5
	2.0019	2.0006	2.0001	−38.8
	2.0018	2.0007	2.0001	−39.5

[a]Reference 37.

[b]Calculated values at the DFT-B3LYP/6-31G(d) level are shown for all the positively charged clusters investigated in this work.

ionizing radiation process creates not only holes but also electrons. If the electrical level of resulting hole-trapping centers is rather low, these centers will tend to capture electrons and return to the corresponding neutral species. On the other hand, the hole-trapping centers with higher electrical levels are more stable against electron trapping and will remain intact during radiation exposure. We hence consider that the BHODC-type defect is more likely to survive the electron capturing process in the course of ionizing radiations because of its high electrical level.

When the BHODC-type defect is created in silica glass by ionizing radiations, this type of defect will show a switching behavior against applied electric fields. Although the electrical level of BHODC is rather high, some of the BHODC defects will be eventually discharged by electron injection under positive bias (electron injection), forming the neutral version of BHODC. Under negative bias (hole injection), on the other hand, the neutral version of BHODC will be positively charged rather easily because of its high electrical level. BHODC can hence switch charge state in response to change in the polarity of the applied electric field, as indeed observed experimentally for E'_γ center.

From the foregoing arguments, we insist that BHOCD configurations may exist in silica glass and they would have properties similar to those observed for E'_γ centers.

V. CONCLUSIONS

In this work, we have investigated structural transformations of the neutral oxygen vacancy during the hole trapping process on the basis of the DFT cluster calculations. As a consequence of the hole trapping at the neutral-oxygen-vacancy site, the positively charged dimer is formed. The present DFT cluster calculations have further demonstrated that the dimer can be relaxed into other positively charged configurations depending on the surrounding environments. When the back oxygen is suitably located behind the dimer site, it will be asymmetrically relaxed into the conventional puckered configuration. The total energy of the clusters with the puckered defect is dependent on the atomic arrangements around the defect. We should note, however, that an alternative asymmetric relaxation can be achieved by the forward-oriented process. In this process, there is no need to assume the existence of a particular oxygen site which is requited to induce the relaxation. We have also shown that the forward-oriented configuration can further be transformed into the structure called the BHODC by appropriate bond switching.

We then evaluate the stability of the above positively charged defects against discharging in terms of the electrical levels. We have found that the electrical level associated with the BHODC and the related neutral species is the highest among the defect configurations investigated in this work. This indicates that the BHODC is the most stable configuration against discharging and is hence likely to be responsible for the E'_γ center. The structural model of the E'_γ center has further been supported by the hyperfine-parameter and g-value calculations performed for the BHODC configuration.

ACKNOWLEDGMENTS

We would like to thank the Supercomputer Laboratory, Institute for Chemical Research, Kyoto University, for providing the computer time. This work was supported in part by Grant-in-Aids (17206068) from the Ministry of Education, Science, Sports, and Culture, Japan, and the Toray Science Foundation.

[1] D. J. DiMaria, in *The Physics of SiO_2 and Its Interfaces*, edited by S. T. Pantelides (Pergamon, New York, 1978), p. 160.
[2] A. Othonos and K. Kalli, *Fiber Bragg Gratings: Fundamentals and Applications in Telecommunications and Sensing* (Artech House, Boston, 1999).
[3] A. J. Lelis, H. E. Boesch, Jr., T. R. Oldham, and F. R. McLean, IEEE Trans. Nucl. Sci. **35**, 1186 (1988).
[4] P. M. Lenahan and P. V. Dressendorfer, J. Appl. Phys. **55**, 3495 (1984).
[5] R. A. Weeks, J. Non-Cryst. Solids **179**, 1 (1994).
[6] D. L. Griscom, J. Non-Cryst. Solids **73**, 51 (1985).
[7] D. L. Griscom, J. Ceram. Soc. Jpn. **99**, 923 (1991).
[8] F. J. Feigl, W. B. Fowler, and K. Y. Yip, Solid State Commun. **14**, 225 (1974).
[9] J. K. Rudra and W. B. Fowler, Phys. Rev. B **35**, 8223 (1987).
[10] D. L. Griscom, Mater. Res. Soc. Symp. Proc. **61**, 213 (1986).
[11] W. L. Warren, P. M. Lenahan, and C. J. Brinker, J. Non-Cryst. Solids **136**, 151 (1991).
[12] J. F. Conley Jr., P. M. Lenahan, A. J. Lelis, and T. R. Oldham, Appl. Phys. Lett. **67**, 2179 (1995).
[13] W. L. Warren, E. H. Poindexter, M. Offenberg, and W. Müller-Warmuth, J. Electrochem. Soc. **139**, 872 (1992).
[14] Z.-Y. Lu, C. J. Nicklaw, D. M. Fleetwood, R. D. Schrimpf, and S. T. Pantelides, Phys. Rev. Lett. **89**, 285505 (2002).
[15] S. Mukhopadhyay, P. V. Sushko, A. M. Stoneham, and A. L. Shluger, Phys. Rev. B **70**, 195203 (2004).
[16] T. Uchino, M. Takahashi, and T. Yoko, Phys. Rev. B **62**, 2983 (2000); **62**, 15303 (2000); Phys. Rev. Lett. **86**, 4560 (2001); **86**, 5522 (2001).
[17] S. Agnello, R. Boscaino, G. Buscarino, M. Cannas, and F. M. Gelardi, Phys. Rev. B **66**, 113201 (2002).
[18] M. Boero, A. Pasquarello, J. Sarnthein, and R. Car, Phys. Rev. Lett. **78**, 887 (1997).
[19] G. Pacchioni, G. Ieranó, and A. M. Márquez, Phys. Rev. Lett. **81**, 377 (1998).
[20] A. Stirling and A. Pasquarello, Phys. Rev. B **66**, 245201 (2002).
[21] T. Uchino, M. Takahashi, and T. Yoko, Phys. Rev. B **64**, 081310(R) (2001).
[22] T. Uchino, M. Takahashi, and T. Yoko, Appl. Phys. Lett. **80**, 1147 (2002).
[23] M. M. G. Alemany and J. R. Chelikowsky, Phys. Rev. B **68**, 054206 (2003).
[24] W. J. Hehre, L. Radom, P. v. R. Schleyer, and J. A. Pople, *Ab initio Molecular Orbital Theory* (Wiley, New York, 1986).

[25] K. Raghavachari, D. Ricci, and G. Pacchioni, J. Chem. Phys. **116**, 825 (2002).
[26] T. Uchino, Curr. Opin. Solid State Mater. Sci. **5**, 517 (2001).
[27] P. V. Sushko, A. L. Shluger, and C. R. A. Catlow, Surf. Sci. **450**, 153 (2000).
[28] A. H. Edwards, P. V. Sushko, A. L. Shluger, and V. B. Sulimov, IEEE Trans. Nucl. Sci. **49**, 1383 (2002).
[29] K. Vollmayr, W. Kob, and K. Binder, Phys. Rev. B **54**, 15808 (1996).
[30] M. S. Gordon, Chem. Phys. Lett. **76**, 163 (1980) and references therein.
[31] *GAUSSIAN 03, Revision B.03*, M. J. Frisch, G. W. Trucks, H. B. Schlegel, G. E. Scuseria, M. A. Robb, J. R. Cheeseman, J. A. Montgomery, Jr., T. Vreven, K. N. Kudin, J. C. Burant, J. M. Millam, S. S. Iyengar, J. Tomasi, V. Barone, B. Mennucci, M. Cossi, G. Scalmani, N. Rega, G. A. Petersson, H. Nakatsuji, M. Hada, M. Ehara, K. Toyota, R. Fukuda, J. Hasegawa, M. Ishida, T. Nakajima, Y. Honda, O. Kitao, H. Nakai, M. Klene, X. Li, J. E. Knox, H. P. Hratchian, J. B. Cross, C. Adamo, J. Jaramillo, R. Gomperts, R. E. Stratmann, O. Yazyev, A. J. Austin, R. Cammi, C. Pomelli, J. W. Ochterski, P. Y. Ayala, K. Morokuma, G. A. Voth, P. Salvador, J. J. Dannenberg, V. G. Zakrzewski, S. Dapprich, A. D. Daniels, M. C. Strain, O. Farkas, D. K. Malick, A. D. Rabuck, K. Raghavachari, J. B. Foresman, J. V. Ortiz, Q. Cui, A. G. Baboul, S. Clifford, J. Cioslowski, B. B. Stefanov, G. Liu, A. Liashenko, P. Piskorz, I. Komaromi, R. L. Martin, D. J. Fox, T. Keith, M. A. Al-Laham, C. Y. Peng, A. Nanayakkara, M. Challacombe, P. M. W. Gill, B. Johnson, W. Chen, M. W. Wong, C. Gonzalez, and J. A. Pople (Gaussian, Inc., Pittsburgh, 2003).
[32] C. Lee, W. Yang, and R. G. Parr, Phys. Rev. B **37**, 785 (1988).
[33] A. D. Becke, J. Chem. Phys. **88**, 1053 (1988).
[34] T. Uchino, M. Takahashi, and T. Yoko, Phys. Rev. Lett. **86**, 1777 (2001).
[35] A. S. Mysovsky, P. V. Sushko, S. Mukhopadhyay, A. H. Edwards, and A. L. Shluger, Phys. Rev. B **69**, 085202 (2004).
[36] D. Donadio, M. Bernasconi, and M. Boero, Phys. Rev. Lett. **87**, 195504 (2001).
[37] D. L. Griscom, Nucl. Instrum. Methods Phys. Res. B **1**, 481 (1984).
[38] A. H. Edwards, W. M. Shedd, and R. D. Pugh, J. Non-Cryst. Solids **289**, 42 (2001).
[39] P. E. Blöchl, Phys. Rev. B **62**, 6158 (2000).
[40] F. Neese, J. Phys. Chem. **115**, 11080 (2001).
[41] R. A. Weeks, J. Appl. Phys. **27**, 1376 (1956).
[42] H. Hanafusa, Y. Hibino, and F. Yamamoto, J. Appl. Phys. **58**, 1356 (1985).